Available online at www.sciencedirect.com
SCIENCE DIRECT®
Journal of Magnetic Resonance 171 (2004) 37–42
JMR Journal of Magnetic Resonance
www.elsevier.com/locate/jmr

Line shapes of multiple quantum NMR coherences in one-dimensional quantum spin chains in solids

S.I. Doronin, E.B. Fel'dman, I.I. Maximov*

Institute of Problems of Chemical Physics, Russian Academy of Sciences, 142432 Chernogolovka Moscow Region, Russia

Received 26 March 2004; revised 13 July 2004
Available online 28 August 2004

Abstract

General formulae for intensities of multiple quantum (MQ) NMR coherences in systems of nuclear spins coupled by the dipole–dipole interactions are derived. The second moments of the MQ coherences of zero- and second orders are calculated for infinite linear chains in the approximation of the nearest neighbor interactions. Supercomputer simulations of intensities of MQ coherences of linear chains are performed at different times of preparation and evolution periods of MQ NMR experiments. The second moments obtained from the developed theory are compared with the results of the supercomputer analysis of MQ NMR dynamics. The linewidth information in MQ NMR experiments is discussed.

Keywords: MQ NMR; MQ spin dynamics; MQ correlators

1. Introduction

Multiple quantum (MQ) nuclear magnetic resonance (NMR) is widely used to investigate size, space dimensionality, and structure of many-spin clusters in solids [1–6]. Although intensities of MQ coherences are dependent on the local dipolar frequencies within the evolution period [1] of the MQ NMR experiment [7], the integrated MQ intensities are used usually to extract physical–chemical information from MQ NMR spectra. The integrated intensities are sufficient to obtain the important information in MQ clustering experiments and the phase-incremented method has been developed [8] to measure the integrated intensities at a high signal to noise ratio. At the same time, line shapes of intensities of MQ coherences can be considered as a source of additional information in many cases.

In this work, the results of a supercomputer analysis of the lineshapes of the intensities of MQ coherences of different orders are presented. The second moments of the lineshapes of MQ coherences of zero- and second orders are calculated both analytically on the basis of the developed method and numerically from the line shapes obtained by the supercomputer analysis of fifteen-spin linear chains. Possible applications of the developed approach are also discussed.

2. Intensities of MQ coherences in MQ NMR experiments

We consider a system of nuclear spins coupled by the dipole–dipole interactions (DDI) in a two-dimensional time-resolved MQ NMR experiment consisting of the four periods: preparation, evolution, mixing, and detection, see Fig. 1 and [1]. In the preparation period the system is exposed to a sequence of pulses which leads to the appearance and the further evolution of MQ coherences. Spin dynamics of the system is described by the

* Corresponding author.
E-mail addresses: feldman@icp.ac.ru (E.B. Fel'dman), iimxv@pro.icp.ac.ru (I.I. Maximov).

1090-7807/$ - see front matter © 2004 Elsevier Inc. All rights reserved.
doi:10.1016/j.jmr.2004.07.017

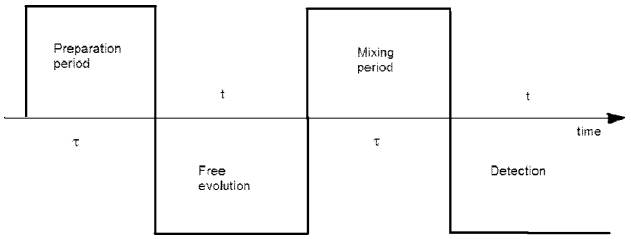

Fig. 1. A schematic presentation of time-domain MQ experiment.

two-quantum/two-spin Hamiltonian, $\mathcal{H}$, during the preparation period of the MQ NMR experiment [1] as follows:

$$\mathcal{H} = \mathcal{H}^{(2)} + \mathcal{H}^{(-2)}, \quad \mathcal{H}^{(\pm 2)} = -\frac{1}{2}\sum_{j<k} D_{jk} I_j^{\pm} I_k^{\pm}, \tag{1}$$

where $I_j^{\pm}$ are the raising and lowering spin angular momentum operators of spin j. The dipolar coupling constant D_{jk} between spins k and j is given by

$$D_{jk} = \frac{\gamma^2\hbar}{2r_{jk}^3}(1 - 3\cos^2\theta_{jk}), \tag{2}$$

where r_{jk} is the distance between spins j and k and θ_{jk} the angle between the internuclear vector $\vec{r}_{jk}$ and the external magnetic field. The sign of the Hamiltonian of the mixing period of the MQ NMR experiments [1] is opposite to that in Eq. (1) and the Hamiltonian, $\mathcal{H}_{\mathrm{dz}}$, of the evolution period is

$$\mathcal{H}_{\mathrm{dz}} = \sum_{j<k} D_{jk}(3I_j^z I_k^z - \vec{I}_j\vec{I}_k). \tag{3}$$

In Eq. (3) I_j^{α} $(\alpha = x, y, z)$ are the spin angular momentum operators. Using the thermal equilibrium density matrix as the initial condition one can obtain the density matrix $\rho(\tau, t)$ after the preparation period of the duration τ, the evolution period t, and the mixing period τ in the high temperature approximation [1] as

$$\rho(\tau, t) = \mathrm{e}^{\mathrm{i}\mathcal{H}\tau}\mathrm{e}^{-\mathrm{i}(\mathcal{H}_{\mathrm{dz}}+\Delta I_z)t}\mathrm{e}^{-\mathrm{i}\mathcal{H}\tau} I_z \mathrm{e}^{\mathrm{i}\mathcal{H}\tau}\mathrm{e}^{\mathrm{i}(\mathcal{H}_{\mathrm{dz}}+\Delta I_z)t}\mathrm{e}^{-\mathrm{i}\mathcal{H}\tau}, \tag{4}$$

where the resonance offset Δ acting during the evolution period is the result of an application of the method of TPPI [1] to separate different MQ orders and $I_z = \sum_i I_i^z$. At the end of the mixing period, the longitudinal polarization, $\langle I_z\rangle(\tau, t)$, is given by

$$\begin{aligned}\langle I_z\rangle(\tau, t) &= \mathrm{Tr}\{\rho(\tau, t) I_z\} \\ &= \mathrm{Tr}\{\sigma(\tau)\mathrm{e}^{-\mathrm{i}(\mathcal{H}_{\mathrm{dz}}+\Delta I_z)t}\sigma(\tau)\mathrm{e}^{\mathrm{i}(\mathcal{H}_{\mathrm{dz}}+\Delta I_z)t}\}\end{aligned} \tag{5}$$

and $\sigma(\tau) = \mathrm{e}^{-\mathrm{i}\mathcal{H}\tau} I_z \mathrm{e}^{i\mathcal{H}\tau}$ is the density spin operator at the end of the preparation period. It is convenient to expand the density spin operator $\sigma(\tau)$ in the series [9,10] as

$$\sigma(\tau) = \sum_n \sigma_n(\tau), \tag{6}$$

where $\sigma_n(\tau)$ is the contribution to the $\sigma(\tau)$ from MQ coherences of the nth order. Substituting Eq. (6) into Eq. (5) yields

$$\langle I_z\rangle(\tau, t) = \sum_n \mathrm{e}^{-\mathrm{i}n\Delta t}\mathrm{Tr}\{\mathrm{e}^{-\mathrm{i}\mathcal{H}_{\mathrm{dz}}t}\sigma_n(\tau)\mathrm{e}^{\mathrm{i}\mathcal{H}_{\mathrm{dz}}t}\sigma_{-n}(\tau)\}. \tag{7}$$

To derive Eq. (7) we took into account the identity

$$\begin{aligned}&\mathrm{Tr}\{\mathrm{e}^{-\mathrm{i}\mathcal{H}_{\mathrm{dz}}t}\sigma_n(\tau)\mathrm{e}^{\mathrm{i}\mathcal{H}_{\mathrm{dz}}t}\sigma_m(\tau)\} \\ &\quad = \delta_{-m,n}\mathrm{Tr}\{\mathrm{e}^{-\mathrm{i}\mathcal{H}_{\mathrm{dz}}t}\sigma_n(\tau)\mathrm{e}^{\mathrm{i}\mathcal{H}_{\mathrm{dz}}t}\sigma_{-n}(\tau)\},\end{aligned} \tag{8}$$

where $\delta_{-m,n}$ is the Kronecker delta function. The normalized intensity of the MQ NMR coherence of the nth order, $F_n(\tau, t)$, is

$$\begin{aligned}F_n(\tau, t) &= \frac{\mathrm{Tr}\{\mathrm{e}^{-\mathrm{i}\mathcal{H}_{\mathrm{dz}}t}\sigma_n(\tau)\mathrm{e}^{\mathrm{i}\mathcal{H}_{\mathrm{dz}}t}\sigma_{-n}(\tau)\}}{\mathrm{Tr}\{I_z^2\}} \\ &= \frac{\mathrm{Tr}\{\mathrm{e}^{-\mathrm{i}\mathcal{H}_{\mathrm{dz}}t}\sigma_n(\tau)\mathrm{e}^{\mathrm{i}\mathcal{H}_{\mathrm{dz}}t}\sigma_{-n}(\tau)\}}{N2^{N-2}},\end{aligned} \tag{9}$$

where N is the number of spins. We shall call the correlation function $F_n(\tau, t)$ as the MQ correlator of the nth order. The Fourier transformation of $F_n(\tau, t)$ with respect to t yields the MQ correlator of Eq. (9) in the frequency domain, $G_n(\omega, \tau)$, and the area $S(\tau) = \int_{-\infty}^{\infty} G_n(\omega, \tau)\,\mathrm{d}\omega$ is

$$\begin{aligned}S(\tau) &= \frac{1}{2\pi}\int_{-\infty}^{\infty}\mathrm{d}\omega\int_0^{\infty}\mathrm{e}^{-\mathrm{i}\omega t}F_n(\tau, t)\,\mathrm{d}t \\ &= \frac{1}{2\pi}\int_0^{\infty}F_n(\tau, t)\,\mathrm{d}t\int_{-\infty}^{\infty}\mathrm{e}^{-\mathrm{i}\omega t}\,\mathrm{d}\omega \\ &= \int_0^{\infty}F_n(\tau, t)\delta(t)\mathrm{d}t = F_n(\tau, 0) \\ &= \frac{\mathrm{Tr}\{\sigma_n(\tau)\sigma_{-n}(\tau)\}}{N2^{N-2}},\end{aligned} \tag{10}$$

where $\delta(t)$ is Dirac's δ-function and $F_n(\tau, 0)$ is called [8] the integrated intensity of the MQ coherence of the nth order. The integrated intensities were calculated exactly in one-dimensional systems (linear chains and rings) in the approximation of the nearest neighbor interactions [9–11]. The developed approach takes the DDI of nuclear spins into account only. At the same time, chemical shift anisotropy may also be important. The theoretical analysis can be generalized easily to the case of the different spin interactions. However, supercomputer calculations are getting more complex and will be accomplished in the future.

3. Supercomputer calculations of MQ correlators in time and frequency domains

We study dynamics of a linear nuclear spin chain consisting of 15 spins coupled by the DDI. The spin density operator of the system at the end of the preparation period of MQ experiment [1] was obtained numerically in [12]. We use the results of [12] as the initial conditions to calculate the spin density operator at the different durations of the evolution period of the MQ NMR experiment [1]. To this end, parallel calculations of the

intensities of MQ coherences at the different times are used as in [12].The computer simulations were performed at the Joint Supercomputer Center of Russian Academy of Sciences. We used MBC-1000M (768 CPU) with the peak performance 1TFlops and 1GByte memory per CPU in the joint supercomputer. This cluster works under LINUX RedHat 6.2 with SMP support. As the result, the MQ correlators $F_n(\tau,t)$ are obtained at the different times τ and t. The intensities of MQ coherences versus the time of the evolution period t for a given preparation time τ are presented in Fig. 2 and can be approximated by Gaussian curves. The calculation grids for the preparation time $\tau = 0.5$ ms and for the evolution time $t = 0.01$ ms were used.

The intensities of MQ coherences of Fig. 2 depend on the time τ of the preparation period. The intensities of MQ coherences of the zeroth and ±second orders are represented on Fig. 3 at different times of the preparation and evolution periods.

Expanding the correlator $F_n(\tau,t)$ in the Taylor series over the time t up to the terms of the fourth order one obtains

$$F_n(\tau,t) \approx F_n(\tau,0) - \frac{t^2}{2} \times \frac{\mathrm{Tr}\{[\sigma_n(\tau),\mathcal{H}_{dz}][\mathcal{H}_{dz},\sigma_{-n}(\tau)]\}}{N2^{N-2}}. \quad (11)$$

It is worth noticing that the correlator $F_n(\tau,t)$ of Eq. (9) satisfies to the condition

$$F_n(\tau,t) = F_{-n}(\tau,t), \quad (12)$$

because of the identities $e^{-i\pi I_x}\sigma_n(\tau)e^{i\pi I_x} = \sigma_{-n}(\tau)$ and $[\mathcal{H}_{dz}, e^{-i\pi I_x}] = 0$. Using Eqs. (9) and (12) one concludes

$$R_n(\tau,t) = \frac{\mathrm{Tr}\{e^{-i\mathcal{H}_{dz}t}[\sigma_n(\tau)+\sigma_{-n}(\tau)]e^{i\mathcal{H}_{dz}t}[\sigma_n(\tau)+\sigma_{-n}\tau]\}}{\mathrm{Tr}\{I_z^2\}} = 2F_n(\tau,t). \quad (13)$$

The symmetrized form $R_n(\tau,t)$ for the correlator $F_n(\tau,t)$ is more convenient to perform the supercomputer calculations. Taking into account the Gaussian approximation for the correlator $F_n(\tau,t)$ which is relevant for the experimental data [1] one can rewrite Eq. (11) as

$$F_n(\tau,t) = F_n(\tau,0)e^{-\frac{1}{2}M_2^{(n)}t^2}, \quad (14)$$

where $M_2^{(n)}$ is the second moment of the MQ coherence of the nth order and

$$M_2^{(n)} = \frac{\mathrm{Tr}\{[\sigma_n(\tau),\mathcal{H}_{dz}][\mathcal{H}_{dz},\sigma_{-n}(\tau)]\}}{N2^{N-2}F_n(\tau,0)}. \quad (15)$$

4. Calculations of the second moments of MQ coherences

The second moments $M_2^{(n)}$ of MQ coherences have been calculated for an infinite linear chain in the approximation of the nearest neighbor interactions when all but the nearest neighbor interactions are set to 0. In that problem the spin density operators $\sigma_n(\tau)$ ($n = 0, \pm 2$) are known exactly [9,10]. In particular, at the end of the preparation period the part of the spin density operator

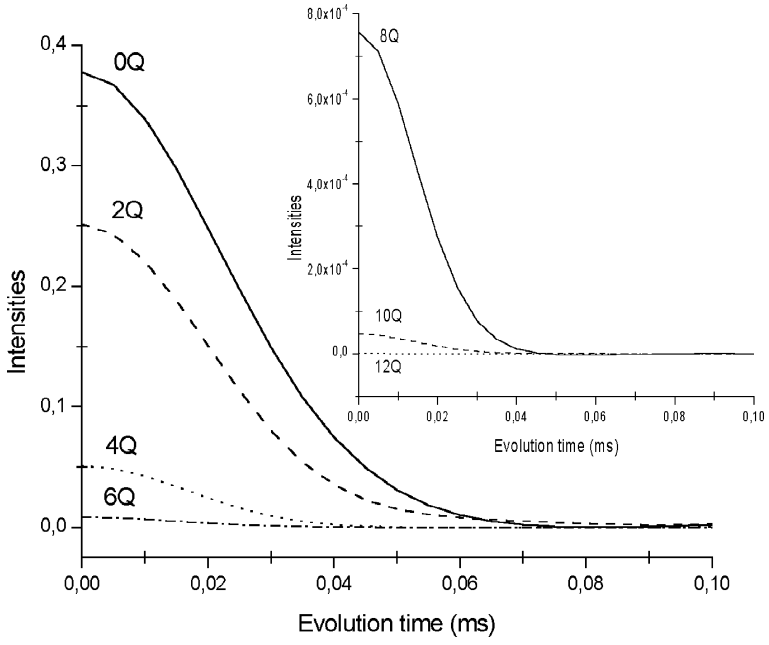

Fig. 2. Intensities of MQ coherences of the zeroth (0Q), second (2Q), fourth (4Q), and sixth (6Q) orders (see Eq. (9)) for a linear chain consisting of 15 spins versus the time of the evolution period; the time of the preparation period is $\tau = 1$ ms. The inset shows MQ coherences of the eighth (8Q), tenth (10Q), and twelveth (12Q) orders. The external magnetic field is directed along the chain. The DDI of the nearest neighbors is $2\pi\cdot 2.95$ kHz.

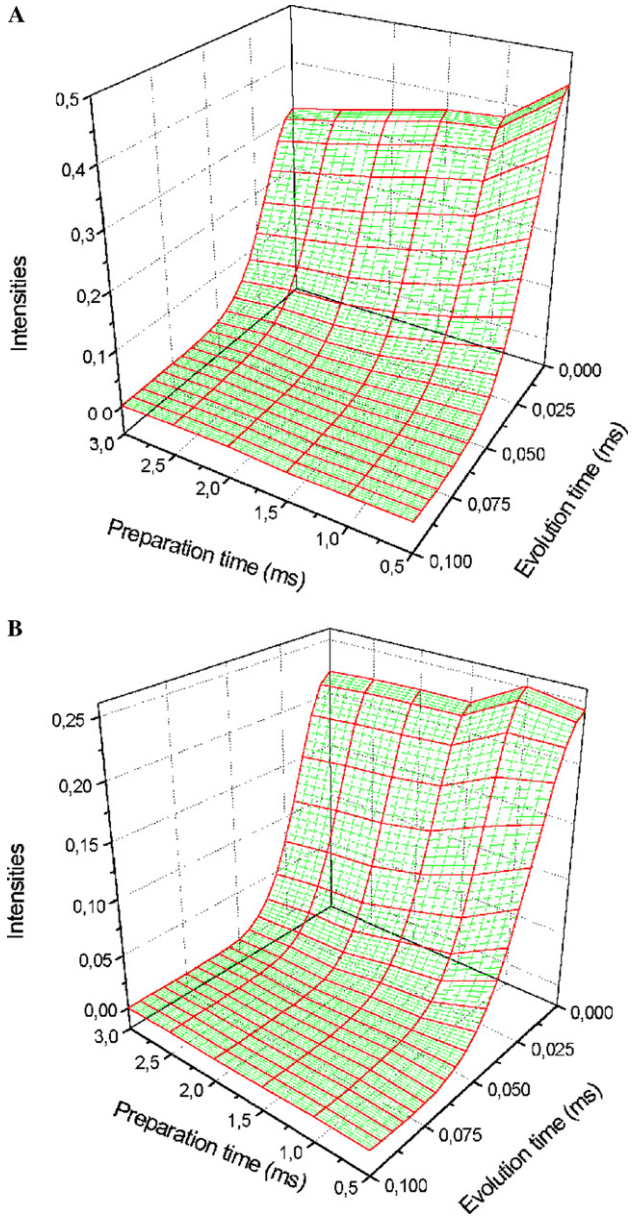

Fig. 3. Intensities of MQ coherences of (A) the zeroth and (B) second orders at different times of the preparation and evolution periods. The external magnetic field is directed along the chain. The DDI of the nearest neighbors is $2\pi\cdot 2.95$ kHz.

$\sigma_0(\tau)$, which is responsible for the MQ coherence of the zeroth order, is

$$\sigma_0(\tau) = \frac{1}{2}\sum_k \cos[2D_{ii+1}\tau \sin k](1 - 2a_k^+ a_k), \tag{16}$$

where $k = \frac{2\pi m}{N}$, with the integer m running $-N/2, -N/2+1, \ldots, N/2-1, N/2$ and N is the total number of spins in the chain; a_k^+, a_k are the fermion raising and lowering operators [10] and $D_{ii+1} \equiv \mathrm{D}$ is the DDI coupling constant of the nearest neighbors ($D = 2\pi\cdot 2.95$ kHz). One can show easily that the flip–flop part of the Hamiltonian $\mathcal{H}_{\mathrm{dz}}$ commutes with the density matrix $\sigma_0(\tau)$ and the calculation of the second moment of 0Q coherence can be reduced to the calculations of the second moment of the MQ coherence of the zeroth order for the zz-part, $\mathcal{H}_{zz}$, of the Hamiltonian $\mathcal{H}_{\mathrm{dz}}$. One obtains

$$\begin{aligned}[\mathcal{H}_{zz}, \sigma_0(\tau)] = -\frac{D}{N}\sum_k \cos[2D\tau \sin k] \\ \times \Bigg\{ \sum_{j+2<j'} 2^{j'-j-3} \times \Big[\mathrm{e}^{\mathrm{i}k(j-j')} I_j^- I_{j'}^+ \\ - \mathrm{e}^{-\mathrm{i}k(j-j')} I_j^+ I_{j'}^- \Big] \Big(I_{j+1}^z \ldots I_{j'-2}^z - I_{j+2}^z \ldots I_{j'-1}^z \Big) \\ + \sum_{j+1<j'} 2^{j'-j-1} \Big[\mathrm{e}^{\mathrm{i}k(j-j')} I_j^- I_{j'}^+ - \mathrm{e}^{-\mathrm{i}k(j-j')} I_j^+ I_{j'}^- \Big] \\ \times I_{j+1}^z \ldots I_{j'-1}^z \Big(I_{j'+1}^z - I_{j-1}^z \Big) \\ + \sum_j \Big[\mathrm{e}^{-\mathrm{i}k} I_j^- I_{j+1}^+ - \mathrm{e}^{\mathrm{i}k} I_j^+ I_{j+1}^- \Big] \Big(I_{j+2}^z - I_{j-1}^z \Big) \Bigg\}. \end{aligned} \tag{17}$$

The sums S_1, S_2, which appear in Eq. (17), are

$$\begin{aligned} S_1 &= \frac{1}{N}\sum_k \cos[2D\tau \sin k] \sin k(j-j'); \\ S_2 &= \frac{1}{N}\sum_k \cos[2D\tau \sin k] \cos k(j-j'). \end{aligned} \tag{18}$$

Changing the variable k to $-k$ one can obtain that $S_1 = 0$. When the limit $N \to \infty$ is performed for S_2 it is possible to replace the summation in Eq. (18) by the integration. As the result, one can find from Eq. (18)

$$S_2 = \begin{cases} 0, & \text{at } j-j' \text{ is odd} \\ J_{2L}(2D\tau), & \text{at } j-j' = 2L, \quad (L \text{ is an integer}), \end{cases} \tag{19}$$

where $J_{2L}(z)$ is the Bessel function of the first kind of order $2L$. Cumbersome but straightforward calculations give

$$M_2^{(0)} = \frac{4D^2}{F_0(\tau,0)}\left[J_2^2(2D\tau) + 2\sum_{L=2,3,\ldots} J_{2L}^2(2D\tau) \right]. \tag{20}$$

Using the relationship for the Bessel functions [13]

$$\sum_{L=1,2,\ldots} J_{2L}^2(2D\tau) = \frac{1}{4}\left[J_0(4D\tau) + 1 - 2J_0^2(2D\tau) \right], \tag{21}$$

the expression for the $M_2^{(0)}$ of Eq. (20) can be written as follows:

$$M_2^{(0)} = \frac{2D^2}{F_0(\tau,0)}\left\{ 1 + J_0(4D\tau) - 2J_0^2(2D\tau) - 2J_2^2(2D\tau) \right\}. \tag{22}$$

The analogous calculations allow one to obtain the second moment $M_2^{(2)}$ of the MQ coherence of the second order which is given by

$$M_2^{(2)} = \frac{1}{F_2(\tau,0)}\left\{D^2\left[1 - J_0(4D\tau) - 2J_1^2(2D\tau)\right] + \frac{1}{\tau^2}\sum_{L=1,2,\ldots} L^2 J_{2L}^2(2D\tau)\right\}. \quad (23)$$

The second moment $\tilde{M}_2^{(2)}$ of the correlator $R_n(\tau,t)$ describing the MQ coherences of plus/minus second order is equal to $M_2^{(2)}$. For the time $\tilde{t}$ which is determined as

$$\tilde{t} = \sqrt{\frac{1}{M_2^{(k)}}}, \quad k = 0, 2 \quad (24)$$

the intensity of the MQ coherence of the kth order ($k = 0, \pm 2$) is diminished approximately by half (see Eq. (14)). One can calculate $\tilde{t}$ with Eqs. (22) and (23). In Table 1 the times $\tilde{t}$ are compared with the analogous times, $\tilde{t}_{sc}$, found from the supercomputer calculations of the MQ coherences of the zeroth order at different durations of the preparation period. The initial values $F_0(\tau,0)$ are taken from the supercomputer calculations [12].

The analogous comparison for the MQ coherence of the second order is represented in Table 2.

Some discrepancies of the numerical results with the analytical ones are explained by an influence of the ends of the 15 spin chain at the numerical calculations and the appearance of MQ coherences of high orders at the supercomputer analysis [12] when the DDI of all spins were taken into account.

The second moments for higher-order coherences cannot be obtained analytically. The numerical results for 4Q and 6Q coherences are shown in Table 3. MQ coherences of higher orders decay faster that 0Q and 2Q ones.

5. Possible applications of linewidth analysis of MQ NMR

If integrated MQ intensities are required only then the linewidth information in MQ NMR experiments is not necessary. In such cases phase incrementation [8] can be applied to provide a sensitive and time-efficient version of MQ NMR. However, the linewidth information in a MQ NMR experiment can be useful. Fig. 4 shows an oscillating dependence of the second moments of the line shapes of 0Q and 2Q coherences on the time of the preparation period for 1D linear chains in accordance with Eqs. (20) and (22). Although the second moments of Eqs. (20) and (22) were obtained in the approximation of the nearest neighbor interactions they are close to the second moments of MQ coherences of linear chains when the DDI of all spins are taken into account. If the regular oscillating dependence of the second moments of the line shapes of 0Q and 2Q coherences was obtained one can conclude that the system under investigation is a 1D one. In hydrogenated amorphous silicon [14] information about the distribution of hydrogen and continuous network of silicon–hydrogen bonds can be extracted from linewidths and lineshapes of MQ coherences. A complex structure of the lineshape in MQ NMR experiments for systems with the DDI and the anisotropic chemical shift is also a source of the

Table 1
Analytical and numerical times of 0Q coherence intensity decay

Preparation time τ(ms)	0.5	1.0	1.5	2.0	2.5	3.0
Initial value $F_0(\tau,0)$ [12]	0.4490	0.3774	0.3699	0.3507	0.3306	0.3147
Supercomputer time $\tilde{t}_{sc} \cdot 10^5$ s (see text)	2.69	2.59	2.40	2.28	2.24	2.16
Time $\tilde{t} \cdot 10^5$ s (see Eq. (24))	2.57	2.40	2.40	2.34	2.26	2.17

Table 2
Analytical and numerical times of 2Q coherence intensity decay

Preparation time τ(ms)	0.5	1.0	1.5	2.0	2.5	3.0
Initial value $F_2(\tau,0)$ [12]	0.2432	0.2514	0.2265	0.2260	0.2239	0.2205
Supercomputer time $\tilde{t}_{sc} \cdot 10^5$ s (see text)	2.76	2.33	2.25	2.12	2.08	2.02
Time $\tilde{t} \cdot 10^5$ s (see Eq. (24))	2.76	2.69	2.51	2.50	2.51	2.53

Table 3
Numerical times of 4Q and 6Q coherence intensity decay

Preparation time τ(ms)	0.5	1.0	1.5	2.0	2.5	3.0
Initial value $F_4(\tau,0)$	0.02989	0.0509	0.0724	0.0781	0.0860	0.0939
Supercomputer time $\tilde{t}_{sc} \cdot 10^5$ s	1.975	1.925	1.905	1.865	1.865	1.855
Initial value $F_6(\tau,0)$	0.0023	0.0082	0.0146	0.0181	0.0219	0.0244
Supercomputer time $\tilde{t}_{sc} \cdot 10^5$ s	1.900	1.750	1.732	1.732	1.750	1.728

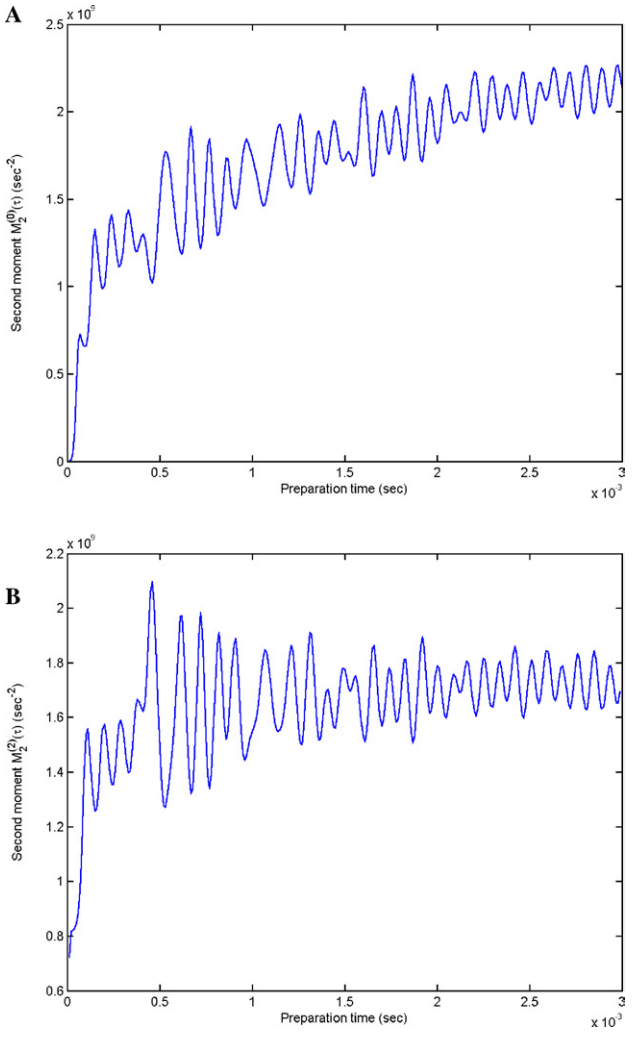

Fig. 4. The second moments of (A) 0Q and (B) 2Q coherences at different times of the preparation period.

valuable information about structural peculiarities in solids. Finally, the lineshapes of MQ coherences of different orders could be very sensitive to molecular movements and the spin–lattice relaxation. The developed technique can be applied with corresponding modifications to the analysis of MQ NMR experiments of the such systems.

Acknowledgment

This work was supported by the Russian Foundation for Basic Research (Grant No. 04-03-32528).

References

[1] J. Baum, M. Munowitz, A.N. Garroway, A. Pines, Multiple-quantum dynamics in solid state NMR, J. Chem. Phys. 83 (1985) 2015–2025.
[2] J. Baum, A. Pines, NMR studies of clustering in solids, J. Am. Chem. Soc. 108 (1986) 7447–7454.
[3] M. Munowitz, A. Pines, Multiple-quantum nuclear magnetic resonance spectroscopy, Science 233 (1986) 525–531.
[4] D.A. Lathrop, E.S. Handy, K.K. Gleason, Multiple-quantum NMR coherence growth in single-crystal and powdered calcium fluoride, J. Magn. Reson. Ser. A 111 (1994) 161–168.
[5] D.H. Levy, K.K. Gleason, Multiple quantum nuclear magnetic resonance as a probe for the dimensionality of hydrogen in polycrystalline powders and diamond films, J. Phys. Chem. 96 (1992) 8125–8131.
[6] R. Tycko, Selection rules for multiple quantum nmr excitation in solids: derivation from time-reversal symmetry and comparison with simulations and ^{13}C NMR experiments, J. Magn. Reson. 139 (1999) 302–307.
[7] G. Cho, J.P. Yesinowski, Multiple-quantum NMR dynamics in the quasi-one-dimensional distribution of protons in hydroxiapatite, Chem. Phys. Lett. 205 (1993) 1–5.
[8] D.N. Shykind, J. Baum, S.-B. Liu, A. Pines, Phase-incremented multiple quantum NMR experiments, J. Magn. Reson. 76 (1988) 149–154.
[9] E.B. Fel'dman, S. Lacelle, Multiple quantum NMR spin dynamics in one-dimensional quantum spin chains, Chem. Phys. Lett. 253 (1996) 27–31.
[10] E.B. Fel'dman, S. Lacelle, Multiple quantum nuclear magneticc resonance in one-dimensional quantum spin chains, J. Chem. Phys. 107 (1997) 7067–7084.
[11] S.I. Doronin, I.I. Maksimov, E.B. Fel'dman, Multiple-quantum dynamics of one-dimensional nuclear spin systems in solids, JETP 91 (2000) 597–609.
[12] S.I. Doronin, E.B. Fel'dman, I.Ya. Guinzbourg, I.I. Maximov, Supercomputer analysis of one-dimensional multiple quantum dynamics of nuclear spins in solids, Chem. Phys. Lett. 341 (2001) 144–152.
[13] M. Abramowitz, I.A. Stegun, Handbook of Mathematical Functions, Dover, New York, 1965.
[14] J. Baum, K.K. Gleason, A. Pines, A.N. Garroway, J.A. Reimer, Multiple quantum NMR study of clustering in hydrogenated amorphous silicon, Phys. Rev. Lett. 13 (1986) 1377–1380.